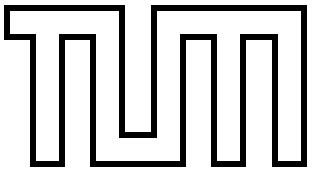

FAKULTÄT FÜR INFORMATIK

DER TECHNISCHEN UNIVERSITÄT MÜNCHEN

Clinical Project

Simulation of CT metal artefacts in C

Author: Alexander Winkler

Advisors: Dipl.-Inf. Philip Stefan,
Dipl.-Inf. Patrick Wucherer,
Pascal Fallavollita, Ph.D.

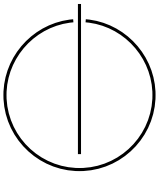

Abstract

Blablabla

Contents

1. Introduction

Almost 100 years ago on April 30th 1917 the Austrian mathematician Johann Radon described in "Über die Bestimmung von Funktionen durch ihre Integralwerte längs gewisser Mannigfaltigkeiten" the mathematical theory computed tomography is based on: He showed that the knowledge of a function $f(x, y)$ in equivalent to the knowledge of all its line integrals. Thus the function can be reconstructed from an infinite set of its projections.[10]

X-Ray is an imaging modality which produces projection images of a volume which show also the internals of the object. So in a perfect world by taking X-Ray images from all angles around an object orthogonal slices of the object can be reconstructed perfectly: In an idealized situation with high radiation dose, monochromatic X-Rays, infinite detector resolution, perfect detectors, no motion and no scatter CT images would be a perfect reflection of reality.[2]

In reality however these conditions are not met. Thus errors in the reconstruction occur resulting in image artefacts.

Usually especially for commercial CT scanners which are used in medical imaging the reduction of these artefacts is of special interest. But to better understand the causes of these artefacts as well as training of medical doctors to make reasonable diagnoses in the presence of these artefacts simulation is also of interest. In this clinical project we developed a simulator of a CT which produces CT images from segmented patient datasets in which the artefacts usually visible in medical imaging are also simulated in a realistic fashion. Especially the simulation of metal artefacts is of major importance as the resulting image artefacts are a major concern in medical imaging as these artefacts degrade image quality considerably.

2. Causes of metal artefacts in CT

2.1. Examples of metal artefacts in CT

To know why metal artefacts in CT should be simulated, we should first know what these metal artefacts are and how they look like.

The human body usually does not contain any metal objects. However many medical implants are composed of metal as well as many surgical tools. Thus metal can indeed be found quite often in patients who are scanned in CT scanners: Artificial hip bones, dental fillings, pacemakers, intramedullary rods, screws or in the case of inerventional CT surgical tools like needles, trocars etc. are found in many patients. If these patients are scanned in CT artefacts in the tomographic reconstruction are usually encountered, how severe these artefacts are depends mainly on their size and the material they are composed of.

These artefacts usually consist of dark stripes between metal objects with light, pin-striped lines covering the surrounding tissue going through the whole or large portions of the reconstruction as can be seen in figure 2.1. Especially in cases in which the radiation is completely absorbed due to the thickness of the materials, very bright strips are found radially around the object with the complete image losing its diagnostic value. More examples can be found in appendix A.

Figure 2.1.: Bilateral hip replacements (with streaks obscuring perirectal lymphadenopathy from rectal cancer)[11]

2.2. Fundamentals of X-Ray physics

To understand the generation of CT metal artefacts we first need to understand how X-Ray generation and attenuation works in general.

2.2.1. Generation of X-Ray radiation[6]

To generate X-Ray radiation an X-Ray tube is used. It consists of a cathode and a rotating anode (usually made of tungsten) which is located within an evacuated tube housing. When electrons from the cathode hit the anode two physical effects take place which result in the emission of X-Ray radiation: Bremsstrahlung and characteristic X-Rays.

Bremsstrahlung results in a continuous spectrum of EM radiation which is produced by the abrupt deceleration of charged particles (”Bremsstrahlung” is German for ”braking radiation”). This deceleration is caused by deflection of electrons in the Coulomb field of the nuclei of the anode material.

Characteristic rays are caused by the removal of inner shell electrons and subsequent filling of the holes with electrons from the outer shells. Shell energy differences determine the energies of the characteristic X-rays (this strongly depends on the anode material).

Both effects together result in the total emission spectrum of the X-Ray source. This spectrum depends on tube voltage and heating current and anode material and anode angle. This spectrum usually looks like as depicted in figure 2.2.

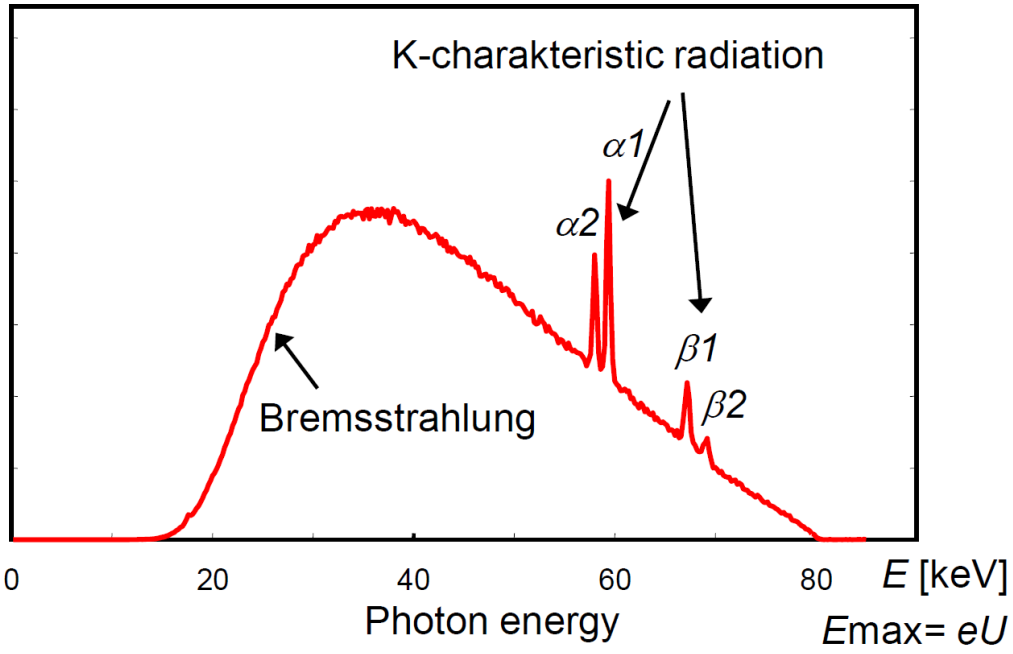

Figure 2.2.: Total X-Ray spectrum of a tungsten anode at an acceleration voltage of U_a = 80kV[6]

2.2.2. Lambert-Beer’s Law[3]

Usually all physical mechanisms that lead to the attenuation of radiation intensity behind a homogeneous object are summed up in a single attenuation coefficient μ. In this simple model the total attenuation of a monochromatic X-Ray beam after passing a distance of $\Delta\eta$ through an object can be calculated as

$$I(\eta + \Delta\eta) = I(\eta) - \mu(\eta)I(\eta)\Delta\eta$$

where I is the radiation intensity - which is proportional to the number of photons.

By reordering and taking the limit $\Delta\eta \to 0$ this leads to the differential quotient

$$\lim_{\Delta\eta\to 0} \frac{I(\eta+\Delta\eta) - I(\eta)}{\Delta\eta} = \frac{\mathrm{d}I}{\mathrm{d}\eta} = -\mu(\eta)I(\eta)$$

If the medium is assumed to be homogeneous the medium can be described by a single attenuation constant $\mu(\eta) = \mu$. By solving this ordinary linear and homogeneous, first-order differential equation with constant coefficients this gives the equation

$$I(\eta) = I_0 e^{-\mu\eta}$$

know as Beer's law of attenuation.

The full derivation of the formula with all assumptions and mathematical intermediate steps can be found in [3].

2.2.3. Beam hardening[3]

X-Ray is colloquially understood to have the property of effectively penetrating material. But from a physical point of view it can be seen that the radiation attenuation is not only dependent on path length but also wavelength dependent and also on the penetrated material.

Thus Lambert-Beer's Law is indeed a simplification. The energy dependence of the attenuation coefficient along the path s also has to be taken into consideration $\mu = \mu(\eta, E)$. This leads to

$$I(s) = \int_0^{E_{\max}} I_0(E) e^{-\int_0^s \mu(\eta,E)\mathrm{d}\eta} \mathrm{d}E$$

where $I_0(E)$ is the X-Ray spectrum.

Reconstruction does not take this non-linear relationship due to the fact that different bands of the frequency spectrum are differently attenuated between the attenuation values, μ, and the measured values of the projection into account thus impairing the reconstruction.

Soft X-ray beams are more strongly absorbed than high-energy, *hard* X-Ray beams. The individual detector elements in practice only measure the integral intensity over all wavelengths, i.e., they cannot differentiate distinct energies. If a non monochromatic X-Ray beam passes through an object different bands of its spectrum are differently attenuated. Without taking this into account in the reconstruction this leads to so called beam hardening artefacts.

The beam hardening effect is especially prominent for metals that are introduced into the human body as their atomic number Z is relatively high with absorption given by

$$\alpha \propto Z^4 \lambda^3$$

(Due to this relationship for example lead (Pb, Z = 82) shields X-ray radiation about 1583 times better than aluminium (Al, Z = 13))

Thus behind a thick metal object the system detects an *infinitely high* attenuation coefficient. Filtered backprojection does not cope with the inconsistencies in the attenuation

values. In the backprojection lines through the object are encountered with extremely high numerical values, which spread across the entire image and are not compensated for by any other projection direction creating star like streaks emanating from the metal object going through the whole or large portions of the reconstruction.[3]

2.3. Fundamentals of CT reconstruction

2.3.1. Sinograms

As described in section 1 the knowledge of all line integrals of *projections* of a function $f(x, y)$ is equivalent to the knowledge of the function itself. With X-Ray being able to create projections of objects opaque to the human eye with this theorem we can create axial slices (or tomographies from $\tau\acute{o}\mu o\varsigma$ *tomos*, "slice, section" and $\gamma\rho\acute{a}\varphi\omega$ *gráphō*, "to write"[15][14][13]) when we take X-Rays from all angles around the object.

An image of all the projections from a line detector of a single slice of an object is called *sinogram* or mathematically Radon transform: In one axis of the image the angle is gradually increased and along the perpendicular line the projection values from the line detector is plotted.

In figure 2.3a the famous Shepp-Logan phantom can be seen created by Larry Shepp and Benjamin F. Logan which serves as a crude model of a human head to develop and test image reconstruction algorithms on. Figure 2.3b is the sinogram of this phantom.[12]

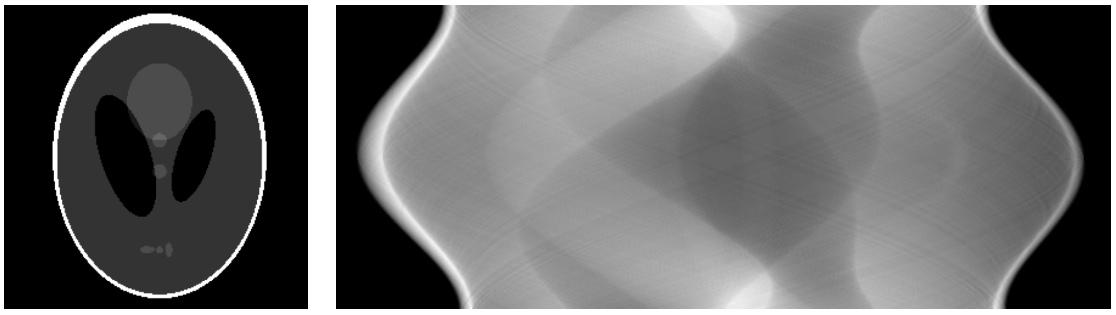

(a) The famous Shepp Logan phantom (own work, based on [12])

(b) Sinogram of the Shepp Logan phantom (own work, based on [12]): In Y direction the projection angle around the object in increased, in X direction the values of the detector are plotted.

2.3.2. Simple Backprojection

To transform such a sinogram from $p_\gamma(\xi)$ back into the image space $f(x, y)$ the basic idea is to *backproject* the values of the detector line along the angle these were acquired from into the image. In the case of *simple backprojection* the would be to *smear back* the values in the direction from which the radiation came. However, although intuitively thsi simple backprojection seems to reverse the process of projection, this procedure does not result in the desired outcome: Due to the fact that the projection $p_\gamma(\xi)$ is a non-negative function, the simple backprojection smears back non-negative values over the entire image, even in areas that were originally (close to) zero. The backprojections from other directions cannot correct these incorrect pixel entries, because the entire set of projections in the sinogram

is a set of non-negative functions. Simple backprojection is visualized in 2.3c and 2.3d showing that it would result in an overall unacceptable blurring of the image.[3]

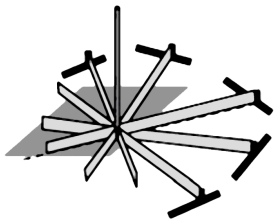

(c) The simple backprojection of a single point...[16]

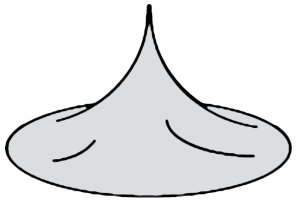

(d) ...would result in the pointspread function of a single point.[16]

2.3.3. Filtered Backprojection

To correct for this unacceptable blurring so called *filtered backprojection* is employed. Today all modern CT systems implement filtered backprojection (and other more advanced reconstruction algorithms). Essentially before backprojecting a high-pass filter is applied. Graphically this can be seen as adding *"negative wings"* to the projections as can be seen in 2.3e and 2.3f. For a mathematical explanation of filtered backprojection and why this is in fact a suitable inversion of the Radon Transform refer to [3].

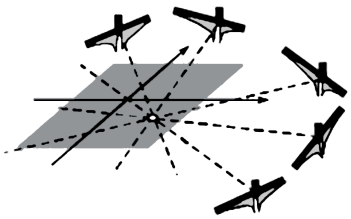

(e) Applying a high-pass filter before projection ...[16]

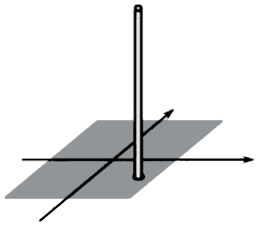

(f) ...results in a crisp reconstruction of the tomography.[16]

Generally the inversion of the Radon transform is an ill-posed problem because the solution is not a continuous function. There are however other techniques for reconstruction, like algebraic and statistical methods and iterative methods.[9][3]

But filtered backprojection is still used in practice as it is computationally fast. Also for our purposes it is the backprojection method of choice as beam hardening and metal artefacts are more prominent than for example in iterative reconstruction.[3]

3. Simulation of CT

In general the simulation of computed tomography consists of two parts: Forward projection and backprojection.

For this clinical project a CT simulator was programmed from ground up in the C programming language without any major libraries like OpenCV, OpenGL or OpenMP. Only standard libraries like `Math.h`, `stdio.h`, `stdlib.h` and the like were included as well as `windows.h` for performance measurements and basic multi threading.

The reason for the decision on C was that originally it was intended to port the code to CUDA-C for calculation on the graphics card to boost performance by multiple orders of magnitude. However due to the lack of time, experience and access to a PC with an NVidia graphics card this port was not completed. Generally the problem seems to be well suited for computation on the graphics card as every forward projection can be calculated in parallel, as well as the filtered backprojection which can also be sped up on the graphics card by a factor of over 200.[1].

The source code for this simulator is available in a git repository hosted at GitHub. It can be found in `https://github.com/Axelius/CTSim.git`

3.1. Forward Projection

The forward projection is in essence a forward Radon Transform with some special conditional statements to simulate effects that exist in physical reality but not in the mathematical model. The simulation especially focuses on the effects of beam hardening, so it simulates a virtual X-Ray tube and has lookup tables for attenuation values of different materials at different tube voltages.

For this simulator basic parallel beam CT was chosen, although today fan beam or cone beam geometry is state of the art. But the artefacts in fan beam geometry should be the same as in parallel beam geometry as fan beam can be converted to parallel beam by simple reordering of the X-Ray beams.[7] In cone beam geometry no central slice theorem exists anyway, so reconstruction is *not mathematically correct anyway* so the simulation of this was not considered[8].

To sum it up the forward projection can be formulated as the formula [4]

3.1.1. Overview over the forward projection

3.1.2. Implementation of line integrals

3.1.3. Implementation of beam hardening

3.2. Back Projection

blabla[1]

3.3. Parts of the simulator

3.3.1. Segmented CT slice

3.3.2. Simulation of X-Ray tube

3.3.3. Look up tables for attenuation values

blabla[5]

3.4. Miscellaneous parts of the simulator

3.4.1. Logger

3.4.2. Image reading and writing

3.5. Future Work

3.5.1. More easily implementable artefacts

Ring artefacts

Poisson noise

Motion artefacts

merging sinogram parts from two simulations, with the moving object at two slightly different positions[4]

3.5.2. Unresolved bugs

4. Results

5. Conclusion

Appendix

A. Real metal artefacts images for reference

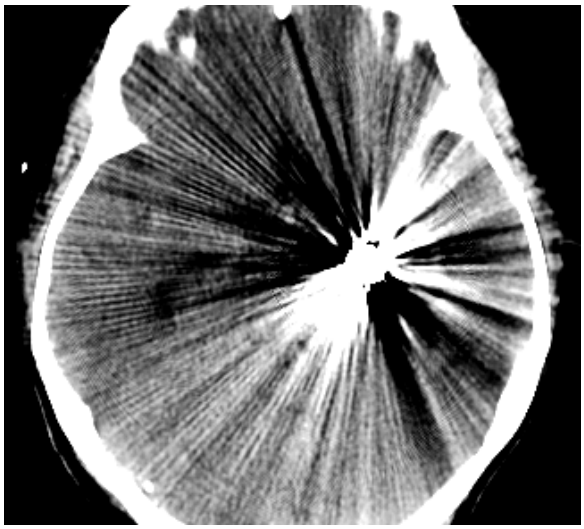

Figure A.1.: Aneurysm clip (with streaks obscuring an acute hemorrhage)[11]

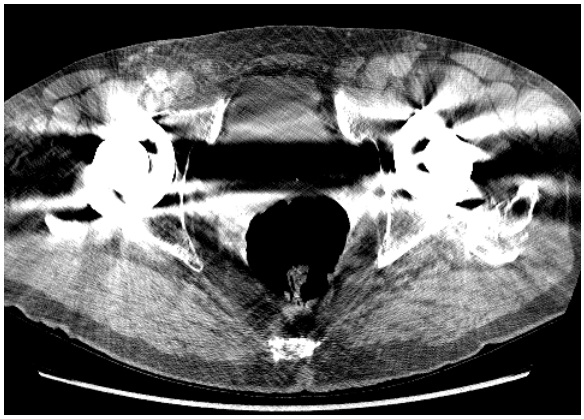

Figure A.2.: Bilateral hip replacements (with streaks obscuring a fluid collection adjacent to the joint)[11]

Figure A.3.: Aneurysm clip (with streaks obscuring an acute infarct)[11]

Figure A.4.: Cholecystectomy clips[11]

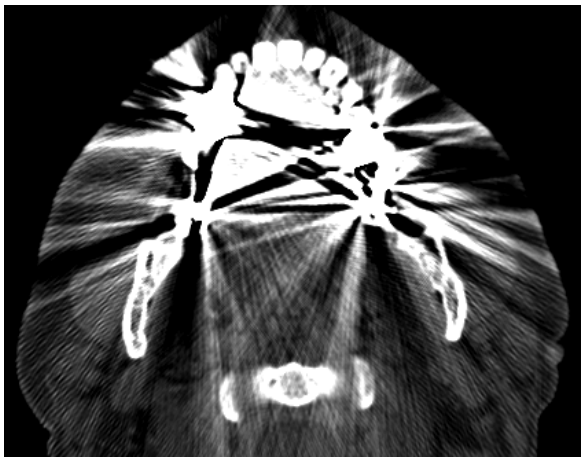

Figure A.5.: Dental fillings[11]

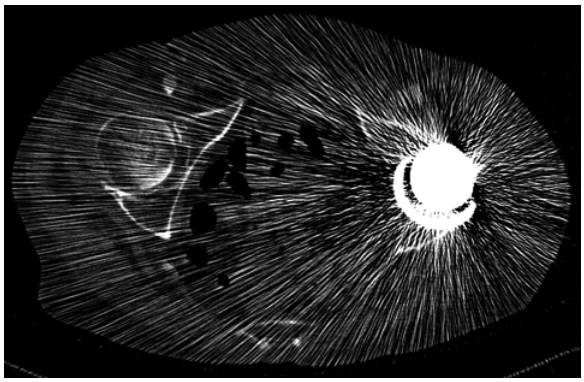

Figure A.6.: Hip replacement[11]

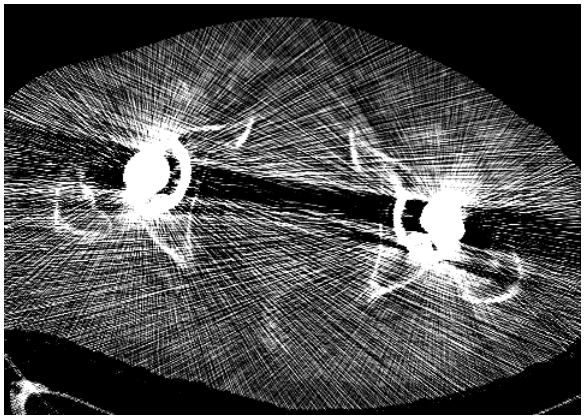

Figure A.7.: Bilateral hip replacements[11]

Figure A.8.: Splenectomy clips[11]

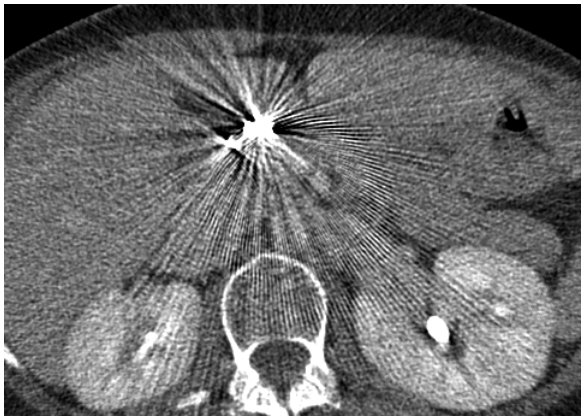

Figure A.9.: Embolization coils[11]

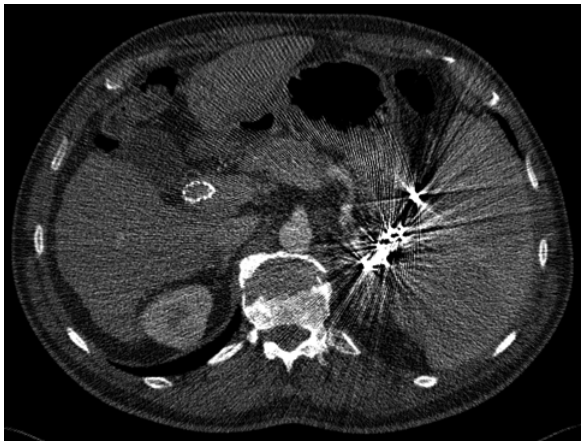

Figure A.10.: Embolization coils[11]

Bibliography

[1] Adam Arnesen. Cuda ct backprojection reconstruction, February 2011. Available online at http://wiki.arnesenfamily.net/doku.php?id=byu:projects:cuda_ct visited on July 30th 2014.

[2] F Edward Boas and Dominik Fleischmann. Ct artifacts: causes and reduction techniques. *Imaging in Medicine*, 4(2):229–240, 2012.

[3] T.M. Buzug. *Computed Tomography: From Photon Statistics to Modern Cone-Beam CT*. Springer, 2008.

[4] Bruno De Man. Iterative reconstruction for reduction of metal artifacts in computed tomography. *status: published*, 2001.

[5] S. M. Seltzer J. H. Hubbell. Tables of x-ray mass attenuation coefficients and mass energy-absorption coefficients from 1 kev to 20 mev for elements z = 1 to 92 and 48 additional substances of dosimetric interest, May 1996. Available online at http://www.nist.gov/pml/data/xraycoef/index.cfm visited on July 30th 2014.

[6] Markus Kowarschik. Interventional Imaging & Image Processing: Angiographic X-ray imaging, Basics of X-ray imaging (generation, absorption, and detection of X-rays). November 2012.

[7] Markus Kowarschik. Interventional Imaging & Image Processing: 2D angiographic imaging. January 2013.

[8] Markus Kowarschik. Interventional Imaging & Image Processing: Flat-detector CT imaging (3D angiographic imaging). January 2013.

[9] A. K Louis. Inverse und schlecht gestellte probleme. *ZAMM - Journal of Applied Mathematics and Mechanics / Zeitschrift für Angewandte Mathematik und Mechanik*, 70(9):409–409, 1990.

[10] Johann Radon. Über die Bestimmung von Funktionen durch ihre Integralwerte längs gewisser Mannigfaltigkeiten. *Akad. Wiss.*, 69:262–277, 1917.

[11] ReVision Radiology. Ct metal artifact reduction using the metal deletion technique (mdt)., February 2014. Available online at http://www.revisionrads.com/index.html visited on August 8th 2014.

[12] L.A Shepp and B.F. Logan. The fourier reconstruction of a head section. *Nuclear Science, IEEE Transactions on*, 21(3):21–43, June 1974.

[13] Wiktionary. -graphy, October 2013. Available online at http://en.wiktionary.org/wiki/-graphy#English visited on August 12th 2014.

[14] Wiktionary. tomo-, December 2013. Available online at `http://en.wiktionary.org/wiki/tomo-#English` visited on August 12th 2014.

[15] Wiktionary. tomography, July 2014. Available online at `http://en.wiktionary.org/wiki/tomography` visited on August 12th 2014.

[16] G. Zeng. *Medical Image Reconstruction: A Conceptual Tutorial*. Higher Education Press, 2010.